Development 133, 251-261 doi:10.1242/dev.02194

The *AUXIN RESPONSE FACTOR 2* gene of *Arabidopsis* links auxin signalling, cell division, and the size of seeds and other organs

Marie C. Schruff[1], Melissa Spielman[1], Sushma Tiwari[1], Sally Adams[2], Nick Fenby[1] and Rod J. Scott[1,*]

Control of seed size involves complex interactions among the zygotic embryo and endosperm, the maternally derived seed coat, and the parent plant. Here we describe a mutant in *Arabidopsis*, *megaintegumenta* (*mnt*), in which seed size and weight are dramatically increased. One factor in this is extra cell division in the integuments surrounding *mnt* mutant ovules, leading to the formation of enlarged seed coats. Unusually for integument mutants, *mnt* does not impair female fertility. The *mnt* lesion also has pleiotropic effects on vegetative and floral development, causing extra cell division and expansion in many organs. *mnt* was identified as a mutant allele of *AUXIN RESPONSE FACTOR 2* (*ARF2*), a member of a family of transcription factors that mediate gene expression in response to auxin. The mutant phenotype and gene expression studies described here provide evidence that *MNT/ARF2* is a repressor of cell division and organ growth. The mutant phenotype also illustrates the importance of growth of the ovule before fertilization in determining final size of the seed.

KEY WORDS: *MEGAINTEGUMENTA*, *AUXIN RESPONSE FACTOR 2*, *Arabidopsis*, Integuments, Ovule, Seed size

INTRODUCTION

Despite the importance of seeds, little is known about the genetic mechanisms that determine their final size and weight. Seed development in flowering plants involves a double fertilization that generates two zygotic products: the embryo, which gives rise to the daughter plant, and the endosperm, which transmits nutrients from the seed parent to the embryo during embryogenesis or germination (Lopes and Larkins, 1993). The third major component of the seed, the seed coat or testa, differentiates after fertilization from maternally derived tissues including the integuments, which enclose the embryo sac. In most monocot species a persistent endosperm forms the bulk of the mature seed, while in most eudicots the endosperm is transient and is replaced by the growing embryo. Therefore, while seed size in monocots such as maize and wheat is often attributable to the extent of endosperm growth (Reddy and Daynard, 1983; Chojecki et al., 1986), in eudicot seeds such as peas and beans, cotyledon cell number has been directly linked to final seed size (Davies, 1975; Davies, 1977). However, in pea, the extent of mitosis in cotyledons is correlated with the extent of invertase activity in the seed coat (Weber et al., 1996), and in the model eudicot *Arabidopsis thaliana*, endosperm proliferation is correlated with seed weight and embryo size, although the mature seed contains only a single layer of endosperm cells (Scott et al., 1998; Garcia et al., 2003). Therefore, in eudicots as well as monocots, the embryo is not the only factor in determining seed size.

The genetic regulation of seed size has been investigated in plants including tomato, soybean, maize, and rice using quantitative trait loci (QTL) mapping. Relatively few loci show significant effects on seed weight in these experiments, and so far none of the corresponding genes have been cloned (Doganlar et al., 2000; Cui et al., 2002; Hyten et al., 2004). In *A. thaliana*, seed weight can vary up to 3.5-fold among accessions (Krannitz et al., 1991), providing an opportunity for QTL analysis of seed size in this species. Alonso-Blanco et al. (Alonso-Blanco et al., 1999) identified 11 loci affecting seed weight and/or length in crosses between the accessions L*er* and Cvi, with the larger size of Cvi seeds attributed mainly to faster and prolonged growth of the seed coat and endosperm.

Mutations and misexpression experiments have revealed few genes affecting seed size. *miniature1* mutants of maize produce small endosperms, and consequently small seeds, due to lesions in a gene encoding a cell wall invertase involved in sugar transport (Cheng et al., 1996). In *Arabidopsis*, the small seed size of *haiku* mutants is correlated with premature arrest of endosperm proliferation; inhibited cell division in the embryo and cell expansion in the seed coat were considered to be indirect effects (Garcia et al., 2003). Mutations in some *TRANSPARENT TESTA* loci, which affect flavonoid pigmentation in the seed coat, also alter seed growth, usually reducing seed weight (Debeaujon et al., 2000). Large seeds in *Arabidopsis* can be generated by mutation of the *APETALA2* (*AP2*) transcription factor (Jofuku et al., 2005; Ohto et al., 2005) or by expression of an antisense DNA methyltransferase gene in the seed parent resulting in DNA hypomethylation (Adams et al., 2000). The size of many organs, including seeds, is increased by ectopic expression of the *AINTEGUMENTA* (*ANT*) transcription factor (Krizek, 1999; Mizukami and Fischer, 2000).

To improve our understanding of the processes controlling seed size, we screened a population of mutagenized *Arabidopsis* for large seeds. We recovered a mutation, now termed *megaintegumenta* (*mnt*), which increases seed size as well as affecting growth of other aerial organs. The earliest difference we detected in *mnt* compared with wild-type seed development was the presence of extra cells in the integuments before fertilization. Many mutants affecting integuments have been identified in *Arabidopsis*, but these usually reduce female fertility (reviewed by Skinner et al., 2004); by contrast, *mnt* mutants are female fertile. Ectopic cell division and/or expansion were also observed in leaves, stems and some floral organs of *mnt* mutants. Cloning of the *MNT* locus showed it to

[1]Department of Biology and Biochemistry, University of Bath, Claverton Down, Bath BA2 7AY, UK. [2]Department of Biology, University of Leicester, University Road, Leicester LE1 7RH, UK.

*Author for correspondence (e-mail: bssrjs@bath.ac.uk)

Accepted 1 November 2005

encode AUXIN RESPONSE FACTOR 2 (ARF2), one of a family of transcription factors that bind to auxin-responsive elements (AuxREs) in the promoters of auxin-regulated genes (Ulmasov et al., 1997; Ulmasov et al., 1999a; Ulmasov et al., 1999b; Liscum and Reed, 2002; Hagen and Guilfoyle, 2002) and possibly other genes (Okushima et al., 2005a; Ellis et al., 2005). Recent studies of *arf2* mutants have reported a pleiotropic phenotype, including: restoration of differential cell elongation and apical hook formation in *hookless1* mutant seedlings; increased growth of aerial organs; inhibition of floral bud opening; and delays in flowering, leaf senescence, floral organ abscission and silique ripening and dehiscence (Li et al., 2004; Okushima et al., 2005b; Ellis et al., 2005). Here we present the first evidence that an ARF is a general repressor of cell division, one of many processes regulated by auxin. The *mnt/arf2* mutant phenotype also illustrates the importance of growth of the ovule before fertilization in determining final size of the seed.

MATERIALS AND METHODS

Plant growth and stocks

Seeds were stratified for 3-5 days at 4°C in 0.15% agar and germinated on Levingtons F2 compost. Plants were grown in a glasshouse at a temperature of 24°C (day) and 17.5°C (night), or in a Sanyo controlled environment room with a daylength of 16 hours, 23°C (day) and 18°C (night). To test for kanamycin resistance, seeds were surface-sterilized and plated on full-strength M+S with Gamborgs Vitamins (Sigma-Aldrich, Dorset, UK), 1% sucrose, 0.8% Phyto Agar (Duchefa, Haarlem, Netherlands), 50 μg/ml kanamycin. Wild-type Col-3 seeds and Col-3 mutagenized with ethane methyl sulfonate (EMS) were obtained from Lehle Seeds (Round Rock, Texas, US). Col-0, L*er*, and Salk_108995 (http://signal.salk.edu/cgi-bin/tdnaexpress) (Alonso et al., 2003) were obtained from the Nottingham *Arabidopsis* Stock Centre (NASC), UK. *mnt* mutants were outcrossed three times to Col-3 before phenotypic analysis.

Pollinations and seed weights

For cross-pollinations, flowers were emasculated before anther dehiscence and pollinated 2-3 days later. For manually pollinated *arf2* mutants, buds were opened early in development to avoid crushing of the stigmatic papillae due to the elongated gynoecium. Seeds were weighed with a Mettler UMT2 microbalance (Mettler-Toledo, Leicester, UK). Statistical analysis was performed with Minitab 12.2 software (State College, Pennsylvania, USA).

Sample preparation and microscopy

For analysis of whole-mount seeds, seeds were dissected from siliques and placed in a drop of clearing solution (8 g chloral hydrate, 11 ml water, 1 ml glycerol). Samples were photographed under a Nikon Eclipse E800 microscope with differential interference contrast optics using a SPOT RT Color camera (Diagnostics Instruments Inc., Michigan, USA). Digital images were processed using Adobe Photoshop software and measurements were taken with Visilog 5.0.2 software (Noesis, Les Ulis, France).

For sections, plant material was fixed overnight at RT in 4% paraformaldehyde, 25 mmol/l $KHPO_4$ buffer pH 7.0, 0.1% Tween-20, washed in buffer, dehydrated through a graded ethanol series to 95% ethanol, and embedded in JB-4 glycol methacrylate resin (Polysciences, Warrington, PA, USA), or dehydrated to 100% ethanol and embedded in Technovit 7100 resin (Heraeus Kulzer, Germany). Five-micrometre sections were cut in ribbons using glass knives made from microscope slides on a Leica RM2145 microtome, according to Ruzin (Ruzin, 1999). Samples were stained in 0.1% Toluidine Blue in 25 mmol/l $KHPO_4$ buffer pH 5.5, mounted under coverslips in DPX (Agar Scientific, Stansted, UK), and photographed under an Olympus BH-2 microscope with a Nikon Coolpix 4500 digital camera. Digital images were processed using Adobe Photoshop software and measurements were taken with Scion Image 4.0.2 software (Scion Corp., Maryland, USA).

For scanning electron microscopy (SEM), siliques were slit open and fixed in 3% glutaraldehyde in 0.05 mol/l sodium cacodylate buffer pH 6.8 overnight at 4°C, postfixed in 1% osmium tetroxide in 0.1 mol/l buffer pH 7.0 for 4 hours at RT, rinsed in buffer, dehydrated through an acetone series, and critical point dried. Ovules were sputter-coated with gold and examined using a JEOL JSM6310 scanning electron microscope (JEOL, Tokyo, Japan).

For confocal laser scanning microscopy (CLSM), Feulgen-stained seeds were processed and imaged as in Bushell et al. (Bushell et al., 2003). GFP fluorescence and chlorophyll autofluorescence were detected in water-mounted samples using an argon ion laser at 488 nm excitation, 505-530 nm emission, and a HeNe543 laser at 543 nm excitation, ⩾585 nm emission, respectively.

For analysis of floral organs, floral buds were photographed under a Leica MZ6 dissecting microscope with a Nikon Coolpix 4500 digital camera. Floral organs were measured using a graticule eyepiece. For analysis of epidermal cells, casts were made of floral organs in clear nail varnish on a microscope slide, and photographed under an Olympus BH-2 microscope as above. Measurements were taken on digital images using Visilog 5.0.2 software.

Statistical analysis was performed with Minitab 12.2 software.

Mapping and sequencing

A recombinant mapping population was generated by crossing *mnt* homozygotes in the Col-3 background with wild-type L*er*. Seven hundred and eighty nine plants with the mutant floral phenotype were selected from the F2 generation and their genomic DNA was scored for published CAPS and SSLP markers (http://www.arabidopsis.org) and for CAPS markers generated in our laboratory (available on request). Genomic and cDNA for sequencing was PCR amplified using proofreading KOD Hi-fi Polymerase (Merck, Nottingham, UK) and cloned into the pGEMT vector (Promega, Southampton, UK). Two independent PCR products were sequenced using internal primers on both sense and antisense strands. Sequences were aligned using Genedoc 2.6.02 software (http://www.psc.edu/biomed/genedoc).

Complementation and allelism test

The region of BAC MTG10 identified by fine mapping as containing the *MNT* locus was restricted with appropriate enzymes to isolate each of the 16 annotated genes. The gel-purified fragments were cloned into shuttle vector ST36 (a modified form of BJ36 in which an *Xba*I-*Spe*I fragment spanning the OCS terminator was removed) and subcloned into the *Not*I sites of binary vector BJ40 (BJ36 and BJ40 were gifts of Bart Janssen, Hort+Research New Zealand). The shuttle vector was transformed into *Agrobacterium tumefaciens* GV3101. *mnt* mutants were transformed via the floral dip method (Clough and Bent, 1998) and T1 seeds were selected on kanamycin as above.

To genotype the Salk_108995 T-DNA insertion mutant, primers 108995-R (5′-CAACTGATGCGTCTCTCCAA-3′) and left border primer Lba1 (5′-TGGTTCACGTAGTGGGCCATCG-3′) were used to identify the T-DNA insertion in the *ARF2* gene. Primers 108995-F (5′-GGGCTCACTGTTTTGCTCAT-3′) and 108995-R were used to identify the wild-type *ARF2* allele in the insertion line. Homozygous insertion mutants were crossed to *mnt* homozygotes and the F1 progeny were assayed for the *mnt* mutant phenotype and hemizygosity for the T-DNA insertion.

pARF2::GFP

A 2.5 kb region of genomic DNA 5′ to the *ARF2* coding region was amplified by PCR using the primers pARF2-F (5′-AAAGTCGAC-ACACAAGAAAATAGAAGAG-3′) and pARF2-R (5′-TCTAGAC-TTAACCAGAGGTAGTCAAAACTC-3′), and cloned into the *Sal*I and *Xba*I sites of the plasmid GFP_DME_NLS (Choi et al., 2002).

Expression analysis

'Young' and 'mature' rosette leaves were harvested from wild-type Col-3, *arf2-8*, and *mnt/arf2-9* plants at 16 and 39 days after germination (dag), respectively. For 'young' stem, primary inflorescence stems were harvested when they reached 5 cm, approximately 29 dag for wild type and up to 32 dag for *arf2* mutants. 'Mature' stem was harvested from plants at 39 dag (wild type) or 43 dag (mutants). For the mature stem base, 10 cm was

measured from the rosette, and for the apex, 10 cm was measured from the cluster of buds at the apex of the inflorescence. All flowers, siliques and axillary shoots were removed from primary inflorescence stems. Total RNA was extracted using TRIZOL (Invitrogen, Paisley, UK).

Five hundred nanograms of total RNA was used for semiquantitative RT-PCR using a Reverse-iT kit (Abgene, Epsom, UK) following the manufacturer's instructions. GapC was used as an internal control. Primers and PCR conditions were: ARGOS (At3g59900), forward 5′-ATCC-TCTGTTTCTGAATCGTGGG-3′ and reverse 5′-ATGCCGTTAGACCA-ACCAATAGG-3′ (26 cycles, annealing temperature 62°C); ANT (At4g37750), forward 5′-ATGAAGTCTTTTTGTGATAATGATG-3′ and reverse 5′-TTGTGTTGTTGTGATGGGTCC-3′ (26 cycles, annealing temperature 55°C); CYCD3;1 (At4g34160), forward 5′-CAAGATT-TGTTCTGGGAAGATG-3′ and reverse 5′-CAATGGAGGTTGTTGCTGC-3′ (27 cycles, annealing temperature 56°C); GAPC (At3g04120), forward 5′-CACTTGAAGGGTGGTGCCAAG-3′ and reverse 5′-CCTGTTGTCG-CCAACGAAGTC-3′ (22-24 cycles, annealing temperature 62°C).

RESULTS

Identification of the *mnt* mutant

In a screen for mutations affecting seed size, approximately 77,000 M2 seeds from an EMS mutagenized population in the Col-3 accession were sieved through a gradient of wire meshes with different apertures (S. A. Adams, PhD Thesis, University of Bath, 2002). Seeds from wild-type controls were retained only in 250-and 300-μm aperture meshes while the mutant seeds were retained in a broader range, from 200 to 355 μm. Inheritance of the phenotype in candidate seed size mutants was tested by weighing seed from M3 plants. A parental group producing seeds larger than controls (Fig. 1A,B), and also containing larger embryos (Fig. 1C,D) was selected for further study; this line was later named *megaintegumenta* (*mnt*) to reflect increased size of the integuments (see below). Apart from the seed phenotype, *mnt* mutants have a variety of abnormalities in vegetative and reproductive development (see below), including failure of flowers to open. This trait was found to co-segregate with the large seed phenotype and was subsequently used for scoring mutant plants. The *mnt* floral phenotype segregates as a single gene recessive mutation (62 wild-type and 23 *mnt* mutant plants were scored in F2 populations following crosses between wild-type and mutant parents; for a 3:1 segregation χ^2=0.192, P>0.05).

Adult *mnt* mutants have a pleiotropic phenotype: inflorescence stems are thick and twisted; plants flower approximately 1 week late with more rosette leaves than wild-type plants grown simultaneously under long day conditions, and the leaves are larger (Fig. 1E; see also below). The mutants have a low degree of self-fertility associated with the failure of floral bud opening (Fig. 1F,G), but female fertility is normal following manual crosses with either *mnt* or wild-type pollen parents, indicating that self-sterility is due to mechanical failure of pollination. However, the last few flowers on a mutant plant self-pollinate and set seed (not shown).

The seed cavity in *mnt* seeds is larger throughout development but endosperm is not hypertrophic

Growth of *mnt* and wild-type seeds was compared by measuring cleared seeds at different stages (Fig. 2A-J; see Table S1 in the supplementary material). Seeds produced by homozygous *mnt* mutants were longer, wider and more pointed at the micropylar pole, with a larger seed cavity, than wild-type seeds at every stage examined. At 5 days after pollination (dap), wild-type seeds had reached the heart stage of embryogenesis, the chalazal endosperm formed a compact rounded cyst, and the peripheral endosperm was cellularizing from the micropylar pole (Fig. 2K, left). At the same

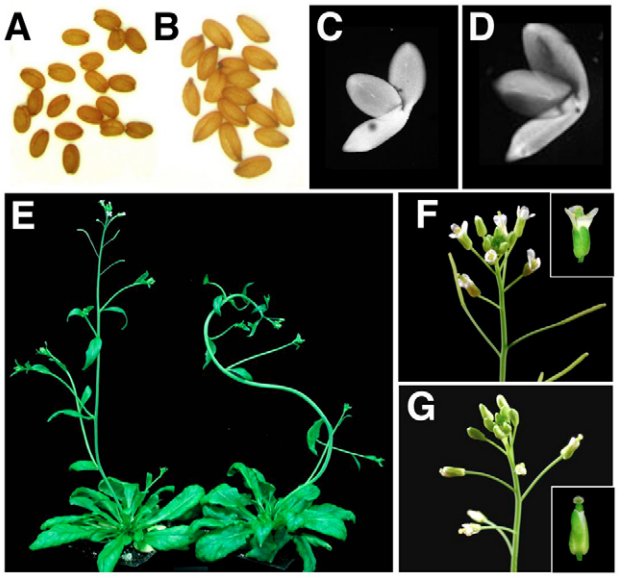

Fig. 1. Pleiotropic effects of the *mnt* mutation. (A-D) Mature seeds (**A**,**B**) and embryos (**C**,**D**) from self-pollinated wild-type Col-3 (A,C) and *mnt* mutant plants (B,D). (**E**) Wild-type (left) and *mnt* (right) plants, showing the *mnt* stem phenotype. (**F**,**G**) Inflorescences from wild-type (F) and *mnt* plants (G); insets show flowers at similar stages.

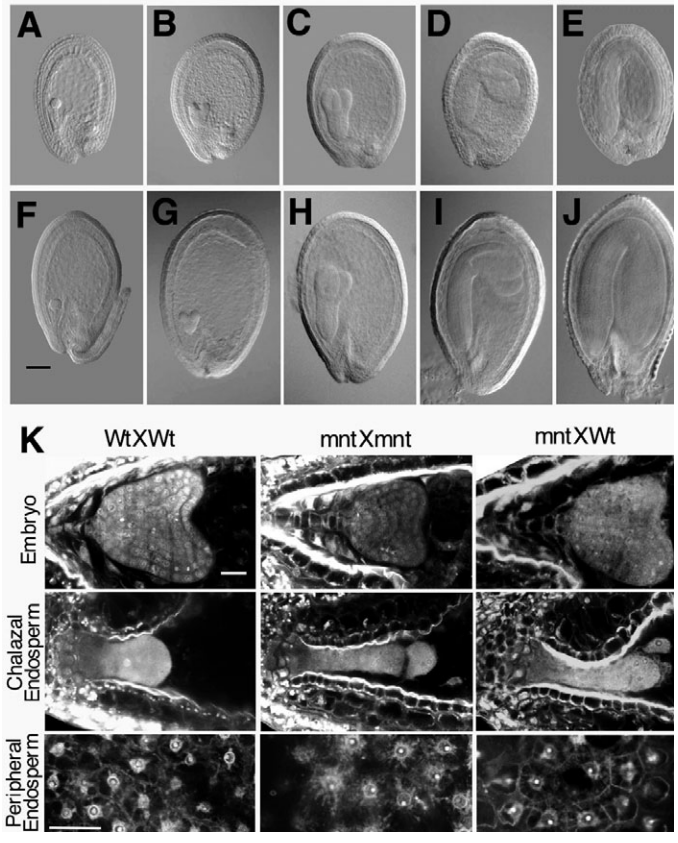

Fig. 2. Seed development in wild-type and *mnt* mutant plants. (**A**-**J**) Cleared seeds imaged with differential contrast optics; (A-E) wild-type and (F-J) *mnt* seeds at similar stages of embryogenesis. Scale bar: 100 μm. (**K**) CLSM images of Feulgen-stained seeds at 5 dap. Scale bars: 20 μm in embryo and chalazal endosperm; 25 μm in peripheral endosperm.

time point, *mnt* homozygous seeds had globular to early heart stage embryos, and the chalazal endosperm was long and thin, presumably due to the abnormal shape of the seed coat (Fig. 2K, middle). Peripheral endosperm did not appear substantially different from wild type. Heterozygous seeds from a cross between an *mnt* homozygous mutant seed parent and a wild-type pollen parent also had the *mnt* mutant phenotype (Fig. 2K, *right*), indicating a maternal effect on seed development.

In *Arabidopsis*, large seeds resulting from an increased ratio of paternal to maternal genomes in the seed ('paternalized'), or DNA hypomethylation of the seed parent, show characteristic endosperm phenotypes, including delayed cellularization of the peripheral endosperm and hypertrophy of the chalazal endosperm and associated nodules (Scott et al., 1998; Adams et al., 2000). There was not a strong trend of late endosperm cellularization in *mnt* mutants. We measured the maximum cross-sectional area of the chalazal cyst plus nodules at 6 dap, a stage at which differences are apparent between wild-type and paternalized endosperms (Scott et al., 1998). Mean areas were 2690 μm^2 (±s.e.m. 328) for wild-type seeds (n=4) and 2537 μm^2 (±416) for *mnt* seeds (n=5), and there was no significant difference between the mutant and wild-type endosperms (two-tailed Student's t-test, P=0.79). Therefore, we concluded that *mnt* endosperms do not have the overgrowth phenotype associated with paternal excess. However, it is possible that eventually more cells are formed in the peripheral endosperm of *mnt* seeds to fill the larger seed cavity.

The increased volume of *mnt* mutant ovules is due to extra cell division in the integuments

As *mnt* mutant seeds were larger than wild-type even at the earliest stage examined, we next compared ovule development in mutant and wild-type plants to investigate the origins of the size difference. Ovule development has been described in detail for *Arabidopsis* (Schneitz et al., 1995; Baker et al., 1997). Early in ovule formation three regions are defined along the proximal-distal axis: the funiculus, which connects the ovule to the mother plant; the chalaza; and the nucellus, which harbours the megaspore mother cell and later the embryo sac. The inner and outer integuments initiate on the flanks of the chalaza and elongate to enclose the nucellus. The integuments divide to a greater extent on the abaxial side, contributing to the curvature of the ovule.

Both *mnt* and wild type followed the pattern previously described for nearly the entire duration of ovule development (Fig. 3A-F; later stages not shown). Female gametophyte development in *mnt* mutants also appeared normal, culminating in a Stage 3-VI embryo sac [staging according to Schneitz et al. (Schneitz et al., 1995)] (Fig. 3G,H). However, at this stage *mnt* mutant ovules were larger and more curved than wild type and the integuments contained more cells in each layer, as well as a partial extra layer in some ovules (Fig. 3H, arrow).

Two layers of the abaxial integuments were examined in more detail: oi2, the outer layer of the outer integument; and ii1', a layer of the inner integument that spans part of the embryo sac (Schneitz et al., 1995; Beeckman et al., 2000). For both layers, *mnt* integuments were longer and contained significantly more cells than wild-type Col-3 (Fig. 3I,J; Table 1). We measured cell length along the proximal-distal axis; for layer ii1' the cell width (abaxial-adaxial axis) was also measured, as cell expansion in this layer coincides with seed growth after fertilization (Beeckman et al., 2000) (Fig. 3K, Table 1). There was no significant difference between wild type and mutant in cell lengths or widths (Table 1). The above evidence indicates that the greater size of integuments in *mnt* ovules is due to extra anticlinal cell divisions in both inner and outer integuments. We also observed extra cells in *mnt* mutant seed coats (data not shown). The pointed shape of *mnt* mutant seeds appears to be due to extension of the seed coat at the micropylar pole combined with overgrowth of the adaxial layers of the seed coat.

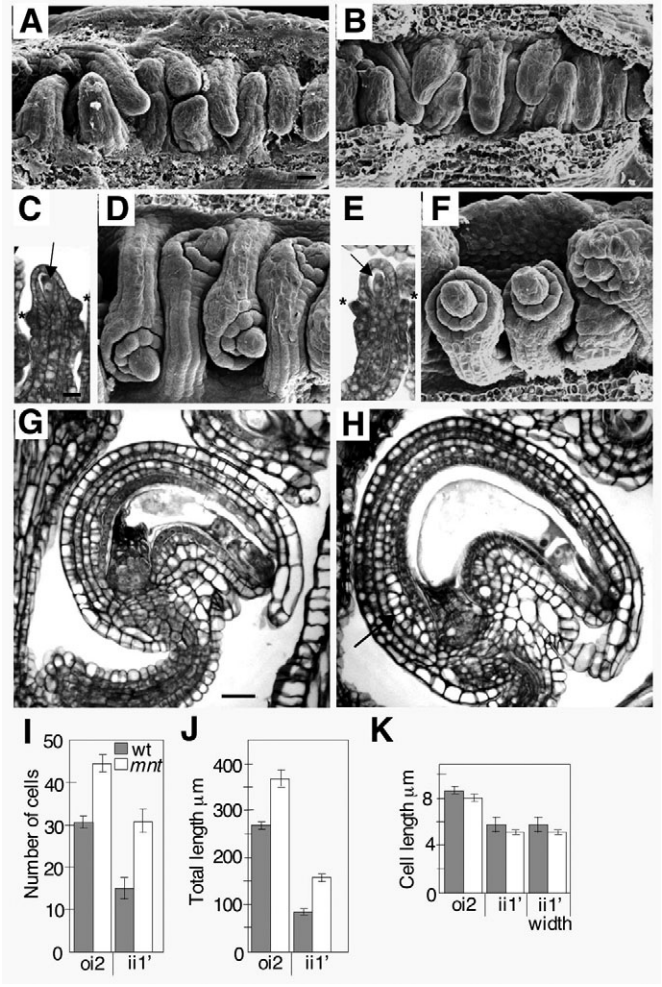

Fig. 3. Ovule development in wild-type and *mnt* mutant plants. (**A-F**) Early ovule development in wild type (A,C,D) and *mnt* (B,E,F). (A,B) SEMs of stage 1-II ovules. (C,E) Sections of stage 2-III ovules showing megaspore mother cell (arrow) and initiating inner integument (*). (D,F) SEMs of later stage 2 ovules showing integuments beginning to extend over nucellus. (**G**,**H**) Sections of mature wild-type (G) and *mnt* (H) ovules. The arrow in (H) shows an extra cell layer. Scale bars: 10 µm in A-F; 20 µm in G,H. (**I-K**) Comparison of number of cells (I), total length of integument (J) and mean size of cells (K) in the abaxial oi2 and ii1' layers of wild-type and *mnt* integuments. Error bars: s.e.m. n=4 wild type, 8 *mnt*.

Factors affecting seed size in *mnt* mutants

To investigate seed weight in *mnt* mutants, we carried out four sets of crosses – [wild type × wild type], [wild type × *mnt*], [*mnt* × *mnt*], [*mnt* × wild type] – using two treatments for each. In the first treatment, six flowers on each primary inflorescence of five plants were manually pollinated and all other flowers on the primary shoot were removed, although the secondary inflorescences were allowed to set self-seed. Due to the poor self-fertility of *mnt* mutants, wild-type seed parents formed many more siliques on secondary

Table 1. Number and size of cells in abaxial integuments of stage 3-VI ovules

	oi2	ii1	ii1′
Number of cells			
Wild type	30.5±1.4	21.5±2.5	15.0±2.0
mnt	44.4±2.2	40.6±2.6	30.8±1.9
P	0.0020	0.0009	0.0004
Total length (μm)			
Wild type	270.8±7.1	126.3±4.9	85.1±7.8
mnt	368.4±18.5	193.2±10.1	158.3±11.1
P	0.0049	0.0011	0.0014
Mean cell length (μm)			
Wild type	8.9±0.3	6.1±0.6	5.8±0.5
mnt	8.2±0.2	4.8±0.2	5.2±0.3
P	0.061	0.030	0.33
Mean cell width (μm)			
Wild type			4.3±0.3
mnt			4.7±0.2
P			0.30

Data represent mean±s.e.m.
n=4 ovules for wild type, *n*=8 ovules for *mnt*.
For Student's *t*-tests, H_0 wild type≠*mnt*.

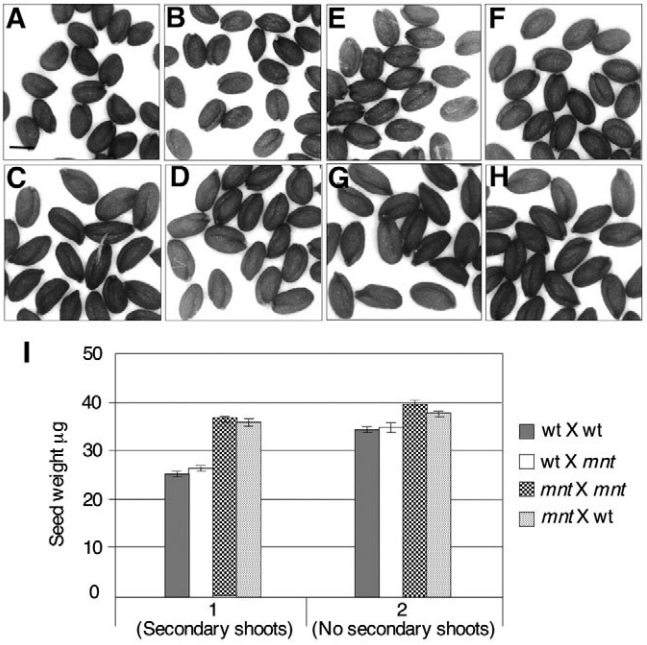

Fig. 4. Comparison of seeds generated by wild-type and *mnt* mutant plants. (**A-D**) Seeds from pollinations where all secondary shoots were allowed to set seed; (**E-H**) seeds from pollinations where secondary shoots were removed (see text). (A,E) [wild type × wild type]; (B,F) [wild type × *mnt*]; (C,G) [*mnt* × *mnt*]; (D,H) [*mnt* × wild type]. Scale bar: 250 μm. (**I**) Comparison of seed weights following the two treatments. Error bars: s.e.m.

inflorescences. Therefore, in order to control for the influence of seed number on seed weight, for the second treatment all secondary inflorescences were removed, so that wild-type and mutant seed parents set the same number of siliques overall.

We found that the genotype of the seed parent is a factor in the overall size, shape and weight of the seed. For both treatments, [*mnt* × *mnt*] and [*mnt* ×wild type] seeds were larger and more pointed than seeds from crosses using a wild-type mother (cf. Fig. 3A,B,E,F and Fig. 3C,D,G,H). [*mnt* × *mnt*] seeds generated by Treatment 1 ('Secondary shoots') were 46% heavier than [wild type × wild type], and [*mnt* × wild type] 35% heavier than [wild type × *mnt*]. However, the weight difference between the two classes decreased when seed set was restricted by removing secondary shoots (Fig. 4I; Table 2A); for example, Treatment 2 ('No secondary shoots') raised [*mnt* × *mnt*] seed weight by 9% while [wild type × wild type] seed weight increased by 36%. However, although increasingly restricted seed set narrowed the gap between them, [*mnt* × *mnt*] seed was still 16% heavier than [wild type × wild type], and this difference was significant (Student's *t*-test, H_0 *mnt*>wild type, *P*=0.0002). We subsequently identified another allele of *mnt*, the T-DNA insertion allele *arf2-8* (see below), and incorporated this allele in two repetitions of the seed weight assay using Treatment 2 and self-pollinations only (Table 2B,C). In each of these replicates both *mnt* and *arf2-8* mutant plants produced significantly heavier seeds (*P*<0.0005) than wild-type (Table 2B,C), with *arf2-8* seeds weighing up to 21% more than wild type even when seed set was severely restricted to control for the reduced fertility of the mutants. We concluded that the difference in seed weights observed between self-pollinated *arf2* mutants and wild-type plants is likely to have two components: direct effects of the mutations on seed development, and an indirect effect due to low self-fertility of the mutants. For both *arf2* alleles tested, in three separate experiments homozygous mutant plants produced significantly heavier seeds than wild-type controls even when the number of siliques on each plant was held constant.

Floral and vegetative development in *mnt* mutants

To investigate the failure of flower opening and self-pollination in *mnt* mutants, we compared floral buds from *mnt* and wild-type plants (Fig. 5A). Mutant inflorescences contain more buds at each stage. At stage 13 (Smyth et al., 1990), when wild-type flowers open, the petal blades have extended above the sepals and reflexed,

Table 2. Seed weights in wild-type and mutant plants

A					B			C		
	Wild type × wild type	Wild type × *mnt*	*mnt* × *mnt*	*mnt* × wild type	Wild type	*mnt*	*arf2-8*	Wild type	*mnt*	*arf2-8*
Secondary shoots	25.0±0.4 μg (*n*=1280)	26.3±0.4 (*n*=705)	36.4±0.6 (*n*=995)	35.4±0.9 (*n*=1171)						
No secondary shoots	34.0±0.6 (*n*=1085)	34.8±1.1 (*n*=978)	39.4±0.7 (*n*=1228, *P*=0.0002)	37.7±0.6 (*n*=1359)	33.4±0.6 (*n*=1287)	37.3±0.5 (*n*=1135, *P*=0.0004)	39.3±0.7 (*n*=1192, *P*=0.0001)	28.2±0.2 (*n*=1506)	32.6±0.6 (*n*=971, *P*=0.0000)	34.1±0.7 (*n*=1112, *P*=0.0000)

Mean weights represent the mean for five plants per cross within each treatment±s.e.m.
n=total number of seeds weighed. *P* represents the P-value obtained from using Student's *t*-test.
H_0 *mnt* or *arf2-8*>wild type.

stigmatic papillae are expanded, the anthers have dehisced, and long stamens are level with the stigma. In *mnt* mutant flowers with expanded stigmatic papillae and dehisced anthers, the gynoecia are longer than the stamens and pollen is shed on the side of the gynoecium in the unopened flower bud rather than on the stigma, explaining the failure of pollination (inset Fig. 5A).

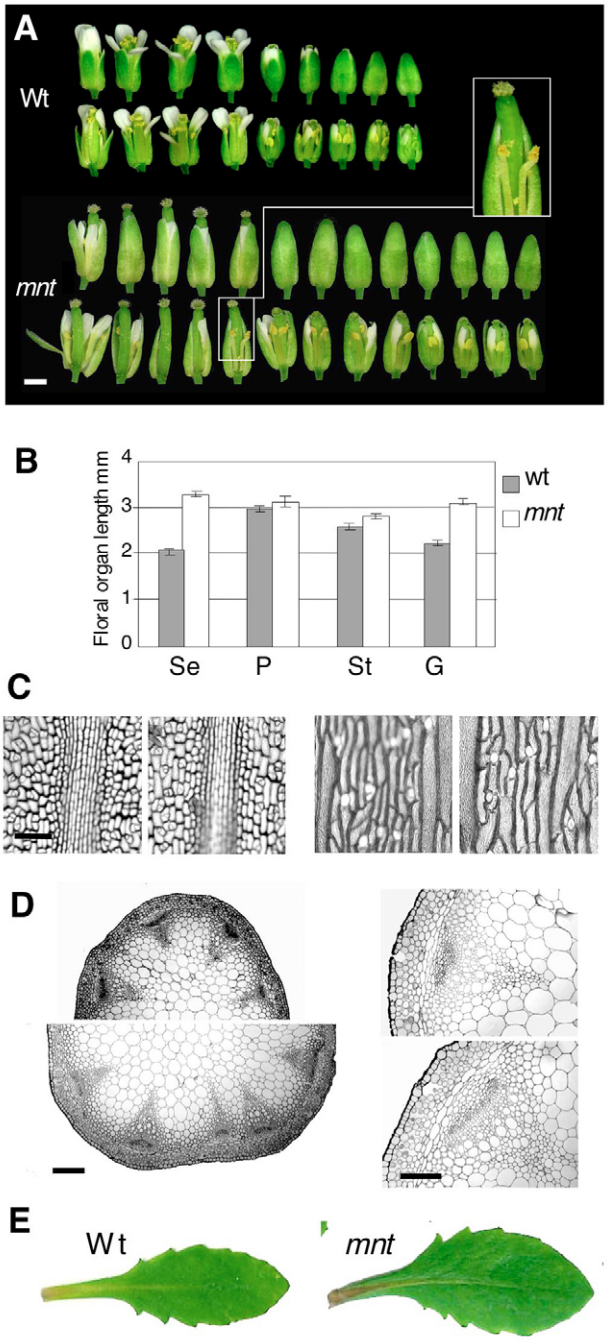

Fig. 5. Floral and vegetative phenotypes of *mnt*. (**A**) Alignment of buds from wild-type and *mnt* inflorescences, approximately stage 12–16. In each part of the figure the bottom row of buds shows the top row partially dissected. (**B**) Lengths of floral organs in stage 13 flowers. (**C**) Nail varnish casts of epidermis from carpel valve (left) and medial sepal (right) of wild-type and *mnt* stage 13 flowers. In each pair the wild type is on the left. (**D**) Transverse sections of inflorescence stem between nodes 2 and 3 from the base: (top) wild-type, (bottom) *mnt*. (**E**) Largest leaf from a wild-type (left) and *mnt* mutant (right) rosette. Scale bars: 1 mm in A; 50 μm in C; 200 μm in D, left; 100 μm in D, right. G, gynoecium (excluding stigma); P, petal; Se, medial sepal; St, long stamen.

We measured the lengths of floral organs in wild-type and *mnt* stage 13 flowers (Fig. 5B; Table 3). Sepals and gynoecia were both significantly longer in the mutant; the resulting disturbance to the petal:sepal and long stamen:gynoecium ratios in *mnt* flowers (Table 3) is consistent with failure of floral opening and pollination. Although the gynoecium length was a consistent factor in failure of self-pollination, in some plants the stamen filaments also failed to elongate fully.

Examination of the epidermal surface of sepals and carpel valves showed that the cells in *mnt* mutants were slightly larger in both organs (Fig. 5C); however, this could not account for the entire increase in size. *mnt* sepals were 60% longer than wild-type (Table 3), but pavement cells in the dorsal sepal epidermis were 32% longer (mean cell length, *mnt* 53.7 μm ± s.e.m. 1.8, n=122 cells in three sepals; wild type 40.8 μm ± 1.8, n=111 cells in three sepals); and *mnt* gynoecia were 42% longer (Table 3), while pavement cells were only 14% longer (*mnt* 26.9 μm ± s.e.m. 1.7, n=113 cells in three carpels; wild type 23.7 μm ± 1.3, n=126 cells in three carpels). We concluded that the increased length of gynoecia and sepals in *mnt* mutants is due to a combination of extra divisions and greater cell expansion.

The diameter of the primary inflorescence stem of wild-type and mutant plants was measured between the first and second nodes from the base when the stems were 15 to 22 cm in length. *mnt* mutant stems had a significantly greater diameter (mean diameter, *mnt* 1.55 mm ± s.e.m. 0.03, n=11; wild type 1.31 ± 0.02, n=10; two-tailed Student's t-test, P=0.0000). Transverse sections of the primary inflorescence stem (Fig. 5D) showed that stem morphology was normal in mutants but there were extra cells of many types. In addition, stem epidermal cells were longer in the mutant (not shown).

mnt mutants produced approximately 30% more rosette leaves than wild-type plants (mean number of leaves per rosette, *mnt* 15.1 ± s.e.m. 0.4, n=14; wild type 11.5 ± 0.5, n=13). In 5-week-old plants we found a significant difference in surface area of the largest leaf (Fig. 5E) (mean area, *mnt* 592.8 mm^2 ± s.e.m. 32, n=14; wild type 440.2 mm^2 ± 22, n=13; two-tailed Student's t-test, P=0.0007). Examination of leaf epidermal cells indicated that, as for sepals, the greater size of *mnt* leaves is most likely due to a combination of extra cell division and expansion (not shown).

mnt is an allele of ARF2

The *MNT* locus was mapped to a 60.9-kb interval on chromosome 5 containing 16 annotated genes on the MTG10 BAC (http://www.arabidopsis.org) (Fig. 6A). Genomic DNA corresponding to the coding region for each gene, along with 5′ and 3′ flanking regions, was transformed into *mnt* mutant plants, and progeny assayed for the wild-type phenotype. Simultaneously, lines with T-DNA insertions in these genes (http://signal.salk.edu) (Alonso et al., 2003) were investigated for similarity to the *mnt* mutant. Homozygous mutants from Salk _108995, which carries an insertion in gene At5g62000, resembled *mnt* mutants in stem, floral and seed phenotype (Fig. 6B; Table 2B,C). An allelism test between *mnt* and Salk_108995 mutants produced F1 plants with the mutant phenotype (Fig. 6B), and the complementation experiment showed that only a genomic fragment including At5g62000 rescued *mnt* mutants (Fig. 6C). Therefore *mnt* is an allele of At5g62000, which encodes ARF2 (Ulmasov et al., 1999a; Li et al., 2004; Okushima et

Table 3. Dimensions of floral organs in wild-type and *mnt* plants

	Medial sepal (mm)	Petal (mm)	Long stamen (mm)	Gynoecium (mm)	Petal/sepal ratio	Long stamen/gynoecium ratio
Wild type	2.06±0.05	2.95±0.08	2.58±0.09	2.20±0.05	1.43±0.03	1.17±0.02
mnt	3.29±0.09	3.12±0.12	2.80±0.09	3.12±0.09	0.95±0.02	0.90±0.01
P	0.0000	0.24	0.095	0.0000	0.0000	0.0000

Data represent mean±s.e.m.
n=10 flowers of each genotype.
P, the *P*-value obtained from using Student's *t*-test. H_0 wild type≠*mnt*.

al., 2005a; Okushima et al., 2005b; Ellis et al., 2005). The Salk_108995 allele was previously designated *arf2-8* (Okushima et al., 2005a); the *mnt* allele is *arf2-9* (Fig. 6D).

We sequenced genomic DNA from *mnt/arf2-9* mutants for the predicted ARF2 coding region plus 4371 bases of the 5′ and 525 bases of the 3′ flanking regions. A single base change with respect to the wild-type Col-0 sequence (http://www.arabidopsis.org), from G to A, was identified at position 665 from translational start, at the end of intron 3. This was predicted to affect splicing by changing the 3′ splice site from the consensus AG sequence to AA. We sequenced the first 837 bases of the *mnt/arf2-9* cDNA from start of translation, and the same region from wild-type Col-3 cDNA, confirming that four bases are deleted from the beginning of exon 4 in the mutant cDNA (Fig. 6E). Based on the cDNA sequence, we predicted the mnt/arf2-9 mutant protein has a frameshift from amino acid position 123 and a premature stop codon at position 167 (Fig. 6F). These changes both occur in the DNA-binding domain of ARF2 (Fig. 6G) and probably cause a complete loss of function.

ARF2 expression in reproductive organs

RNA gel blot analysis has shown that *ARF2* is expressed in roots, leaves, flowers and siliques (Ulmasov et al., 1999b). To investigate the pattern of *ARF2* gene expression in reproductive organs we generated a reporter construct consisting of 2.5 kb of the *ARF2* 5′ flanking sequence fused to a nuclear-localized GFP gene (Choi et al., 2002). Consistent with the *mnt* mutant phenotype, GFP was expressed in floral organs and ovules (Fig. 7A,B). As the ovule matured, expression remained high in the funiculus and gradually declined in the integuments. In mature ovules there was strong signal in the small group of nucellar cells remaining at the chalazal pole (Beeckman et al., 2000) (Fig. 7A, arrow). After fertilization no expression was detected in the seed coat, although signal was seen in embryos dissected from mature seeds (not shown). In floral organs, GFP was observed in the gynoecium at floral stages 8–9 and 12 (Fig. 7B, left), and the signal continued in siliques after fertilization (not shown). GFP was also strongly expressed in other floral organs at stages 8–9, but had largely disappeared by stage 12 (Fig. 7B).

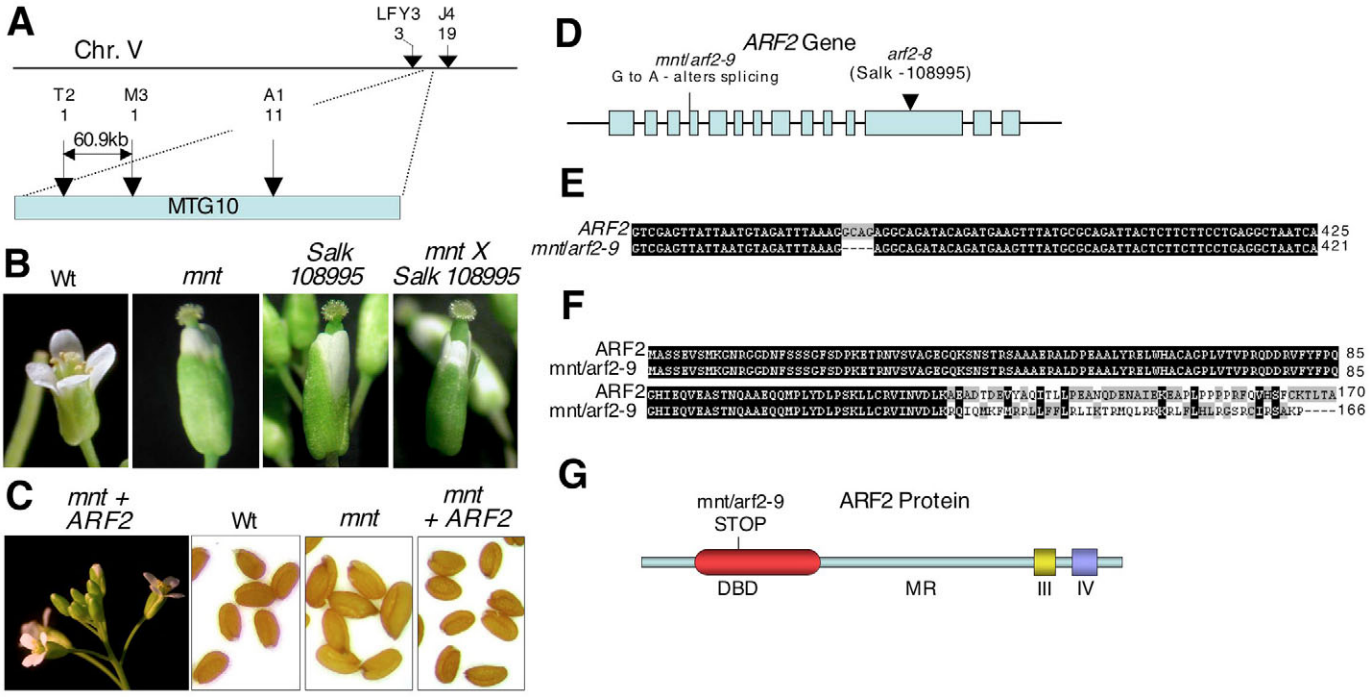

Fig. 6. Mapping and sequencing *MNT*. (**A**) *mnt* mutations were mapped to BAC MTG10 on chromosome V. Figures below the marker names show the number of recombination events in 1578 chromosomes scored. (**B**) Scoring of an allelism test between *mnt* mutants and Salk_108995 T-DNA insertion mutants by floral phenotype. (**C**) Scoring of complementation by floral and seed phenotype. *mnt* + *ARF2*=T1 progeny of an *mnt* mutant transformed with the wild-type *ARF2* gene and flanking genomic DNA. This construct restored wild-type floral (left) and seed phenotypes (right) to the mutant. (**D**) The *ARF2* gene with the positions of the *mnt/arf2-9* and Salk_108995/*arf2-8* mutations marked. (**E**) Alignment of a fragment of wild-type *ARF2* cDNA with the mutated region in *mnt/arf2-9* showing a 4-bp deletion. (**F**) Alignment of the N-terminal portion of the wild-type ARF2 and mutant mnt/arf2-9 proteins, showing an early frameshift and stop codon. (**G**) The ARF2 protein marked with the position of the stop codon generated by the mnt/arf2-9 lesion. DBD, DNA binding domain; MR, variable middle region; III and IV, domains involved in dimerization with other ARFs or with Aux/IAAs (Liscum and Reed, 2002).

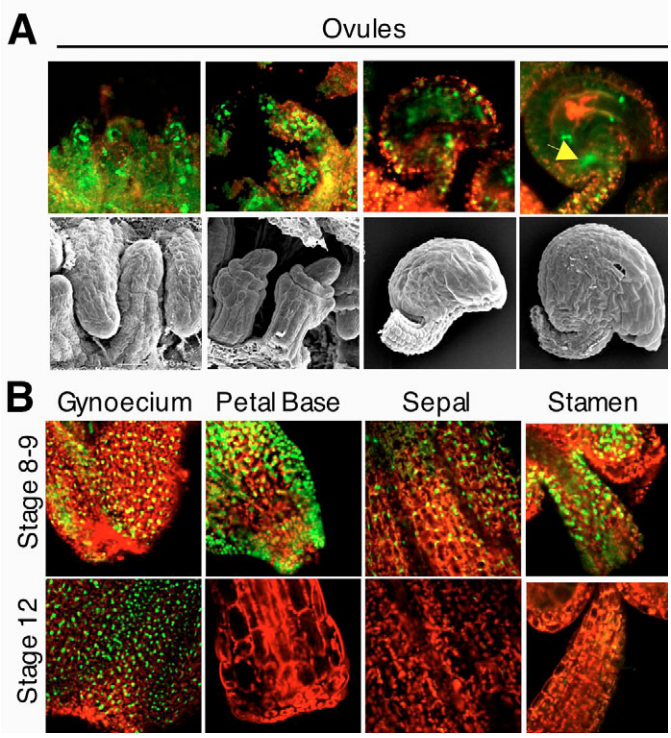

Fig. 7. Expression of nuclear-localized GFP under control of the *ARF2* promoter. (**A**) Expression in ovules; SEMs show ovules at similar stages. (**B**) Expression in floral organs.

Expression of genes promoting cell division is prolonged in *arf2* mutants

It has been proposed that *ANT* is necessary and sufficient to control cell number and growth of lateral organs during shoot development, as loss-of-function *ant* mutations result in small plants with fewer cells, while ectopic *ANT* expression directed by the *35S* promoter results in large organs due to an extended period of cell proliferation (Krizek, 1996; Mizukami and Fischer, 2000). Regulation of the cell cycle by *ANT* is mediated at least in part by prolonging expression of *CYCD3;1*, a D-type cyclin that integrates cell cycle entry with exogenous signals such as hormones, including auxin (Oakenfull et al., 2002): rosette leaves from 9-week-old *35S::ANT* plants continue to express *ANT* and *CYCD3;1*, while expression of both genes in wild-type plants has ceased by this stage (Mizukami and Fischer, 2000). *AUXIN-REGULATED GENE INVOLVED IN ORGAN SIZE* (*ARGOS*), encoding a small protein of unknown function, has similar loss- and gain-of-function phenotypes to those of *ANT,* and also appears to have a role in control of organ size and cell proliferation, acting downstream of auxin signalling and promoting *ANT* and *CYCD3;1* expression (Hu et al., 2003).

Like *35S::ANT* and *35S::ARGOS* plants, *arf2* mutants produce enlarged organs containing extra cells. To investigate whether *ARF2* affects *ARGOS, ANT* or *CYCD3;1* transcription, we assayed expression of these three genes in two organs that show increased cell division in *arf2* mutants, rosette leaves and inflorescence stems (Fig. 8). For young leaves and stems, we found that each gene had similar expression levels in wild-type and mutant plants; this is consistent with previous observations that overexpression of *ARGOS* or *ANT* does not increase expression of *CYCD3;1* in young, dividing tissues (Mizukami and Fischer, 2000; Hu et al., 2003). However, we detected both *ANT* and *CYCD3;1* expression in mature leaves of mutant but not wild-type plants, indicating that loss of *ARF2* function prolongs expression of these genes. In mature stems, these genes were still detectable in wild type but at a lower level than in the mutants. By contrast, *ARGOS* was expressed in mature leaf and stem at similar levels in mutants and wild type.

DISCUSSION

arf2 mutations increase seed size and weight through 'integument-led' seed growth

In a screen for *Arabidopsis* mutants producing large seeds we identified the *mnt* mutant, which contains a lesion in the *ARF2* gene likely to cause complete loss of function. We found that *arf2* mutants generate seeds up to 46% heavier than wild-type seed parents, regardless of the pollination partner. *mnt/arf2-9* seed coats contain more cells than wild type, due to the production of extra cells in the integuments before fertilization (Fig. 3; Table 1). These observations suggest that the *arf2* mutations have a maternal effect on seed size, primarily due to enlarged integuments. However, the reported trade-off between seed number and size in many species (Harper et al., 1970), including *Arabidopsis* (Alonso-Blanco et al., 1999; Meyer et al., 2004), led us to investigate this further by restricting pollination to allow equivalent seed set in wild-type and *arf2* mutant plants. This showed that a component of the difference initially found between *arf2* and wild-type seeds is explained by low seed set in self-pollinated *arf2* plants. Significantly, however, *arf2* mutant seeds were up to 21% heavier than wild type, even when seed set was held constant (Fig. 4; Table 2). Therefore reduced seed set in *arf2* mutants accounts for only part of the increased seed size. Similarly, recent reports show that *ap2* mutations increase seed size partly because of reduced fertility but also through a separate maternal effect on seed growth (Jofuku et al., 2005; Ohto et al., 2005).

Differences between wild-type and *mnt/arf2-9* mutant seeds are apparent before fertilization, and mutant endosperms lack the paternalized phenotype observed in large seeds in which the genetic

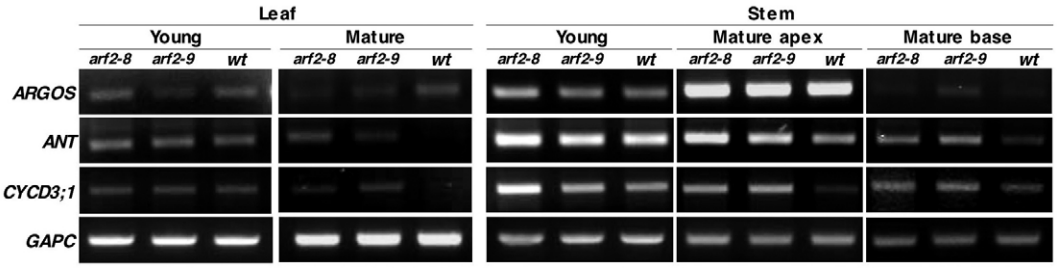

Fig. 8. Comparison of *ARGOS*, *ANT* and *CYCD3;1* transcript levels in young and mature organs of wild-type and mutant plants. See Materials and methods for explanation of developmental staging.

constitution of the endosperm has been altered (Scott et al., 1998; Adams et al., 2000). Therefore, the increased seed size in *arf2* mutants appears to be 'integument-led'. One explanation for integument-led growth is that the larger seed cavity in mutant seeds (Fig. 2) allows greater endosperm growth. Another possibility is that the larger seed cavity provides a greater area of contact for endosperm with the seed coat, leading to increased nutrient uptake.

Mutations affecting integument size often have pleiotropic effects, particularly on flower development (Skinner et al., 2004). *arf2* mutants fit this pattern but are otherwise unusual among integument mutants, as most others reduce female fertility. *aberrant testa shape* (*ats*) and *ap2* mutants are reported to have normal female fertility; however, in these mutants the seed coats are irregularly shaped and display loss of cell layers or structures (Léon-Kloosterziel et al., 1994; Jofuku et al., 1994; Debeaujon et al., 2000). By contrast, the seed coat in *mnt/arf2-9* mutants appears structurally normal, with only a minor effect on shape.

Alonso-Blanco et al. (Alonso-Blanco et al., 1999) reported that growth of the seed coat and endosperm accounted for the larger size of Cvi seeds compared with L*er*, and that as ovules were longer in L*er* than Cvi before fertilization, ovule size differences could not explain the final variation. However, a QTL for seed length was mapped to a region at the bottom of chromosome 5 that contains *ARF2*, and it would be interesting to determine whether *ARF2* corresponds to this locus. Weber et al. (Weber et al., 1996), investigating small- and large-seeded genotypes of broad bean, concluded that the number of cells in the integuments before fertilization could not explain the size differences. The maternal effect of *ap2* mutations on seed size may involve the seed coat (Ohto et al., 2005), but the mechanism for this is not known. Garcia et al. (Garcia et al., 2005) reported that overexpression of the cell cycle inhibitor *KRP2* decreased the number of cells in seed coat without decreasing seed size, and concluded that cell division and cell elongation in the seed coat compensate for each other. However, the effects of increasing cell number in the seed coat were not investigated. The results presented here reveal a mechanism not previously described for increasing seed size within a species, the production of extra cells in the integuments before fertilization.

ARF2 is a general repressor of cell division

The *mnt/arf2-9* mutation causes a variety of phenotypes in the adult plant, including thick stems, large rosette leaves and failure of floral bud opening (Figs 1, 5). These phenotypes were reported for other *arf2* mutant alleles by Li et al. (Li et al., 2004), Okushima et al. (Okushima et al., 2005b) and Ellis et al. (Ellis et al., 2005); here we show they are associated with extra cell division and expansion. Expression of *ARF2* throughout the plant (Ulmasov et al., 1999b) and, within reproductive organs, in floral buds and ovules (Fig. 7), is consistent with the pleiotropy of the mutant phenotype.

Auxin is involved in many processes, including pattern formation, cell division and cell expansion (Leyser, 2002; Vandenbussche and Van Der Straeten, 2004). Single and double mutant phenotypes for other *ARF*s include disturbances to organ patterning, cell expansion or division, response to light or gravity, auxin homeostasis or flower maturation (Berleth and Jürgens, 1993; Sessions and Zambryski, 1995; Liscum and Briggs, 1996; Przemeck et al., 1996; Sessions et al., 1997; Watahiki and Yamamoto, 1997; Hardtke and Berleth, 1998; Stowe-Evans et al., 1998; Harper et al., 2000; Hardtke et al., 2004; Tian et al., 2004; Nagpal et al., 2005; Okushima et al., 2005a; Wang et al., 2005; Wilmoth et al., 2005). We observed that the *mnt/arf2-9* mutation increases cell division in several organs without producing a major effect on morphology, and two mutant alleles of *arf2* had prolonged expression in stem and rosette leaf of *CYCD3;1*, a D-type cyclin involved in cell cycle entry, and *ANT*, a transcription factor involved in organ growth and cell division control. We conclude that ARF2 is a general repressor of cell division in many aerial organs of the plant.

Cell division is not the only process affected by *ARF2*. Li et al. (Li et al., 2004) reported that *ARF2* regulates differential cell elongation in seedlings, and our observations of stem, leaf and floral phenotypes in *mnt/arf2-9* mutants also indicate that *ARF2* plays a role in cell expansion. In addition it has been proposed that *ARF2* promotes developmental transitions such as flowering, floral organ abscission, silique ripening and leaf senescence (Okushima et al., 2005b; Ellis et al., 2005). In this context, extra cell division in *mnt/arf2-9* mutants could result from a delay in transition from the proliferative to the fully differentiated state. Our observations that integument cells in mutant ovules divide for a longer period rather than more rapidly, and that *ANT* and *CYCD3;1* expression is sustained in mature organs rather than increased in young ones, are consistent with this interpretation. However, the timing of cell division and expression of relevant genes need to be investigated in more organs to determine whether extra cell division in *arf2* mutants is generally due to extended proliferation.

Effects of *ARF2* on gene expression

The predominant view of ARFs is that they bind to auxin response elements (AuxREs) in the promoters of auxin-regulated genes, and mediate auxin signalling by activating or repressing gene transcription. It is proposed that auxin influences ARF function through its effects on gene expression and protein turnover of Aux/IAAs, short-lived nuclear proteins that contain AuxREs and are both induced and degraded in response to auxin. Aux/IAAs can dimerize with ARFs, and repress the ability of ARFs to activate gene expression in protoplast transfection assays (Abel and Theologis, 1996; Ulmasov et al., 1997; Leyser, 2002; Liscum and Reed, 2002; Hagen and Guilfoyle, 2002; Tiwari et al., 2003). We found that expression of *ANT* and *CYCD3;1* is prolonged in leaves and stems of *arf2* mutants (Fig. 8), but the mechanism by which this occurs remains to be discovered.

Expression of *ANT* and *CYCD3;1* is also sustained in mature leaves of plants overexpessing *ARGOS* (Hu et al., 2003). *ARGOS* is induced by auxin, and overexpression leads to enlargement of aerial plant organs due to increased cell division (Hu et al., 2003). However, we did not find that *arf2* mutations affected *ARGOS* expression in young or mature organs (Fig. 8), suggesting that *ARF2* does not mediate *ANT* or *CYCD3;1* expression through effects on *ARGOS* expression.

ARF2 represses transcription of reporter genes under the control of synthetic AuxREs both in vitro and in vivo (Tiwari et al., 2003; Li et al., 2004). Surprisingly, *arf2* mutations have not been found to affect global expression of auxin-regulated genes (e.g. *Aux/IAA*s) in seedlings, or expression of specific *IAA* genes in flowers (Okushima et al., 2005b; Ellis et al., 2005). However, there is increasing evidence that *ARF2* affects expression of other types of genes: in addition to prolonging expression of *ANT* and *CYCD3;1* in mature stems and leaves (Fig. 8), loss of *ARF2* function inhibits expression of three members of the *ACS* gene family (involved in ethylene biosynthesis) in flowers (Okushima et al., 2005b) and *SENESCENCE ASSOCIATED GENE 12* (*SAG12*) in senescing leaves (Ellis et al., 2005). It has been proposed that ARF2 does not conform to the canonical auxin response model but may, for example, bind promoters of genes not directly regulated by auxin (the AuxRE motif is highly

represented in the *Arabidopsis* genome), or interact with proteins not directly participating in auxin signalling (Okushima et al., 2005b; Ellis et al., 2005). Identification of the direct targets of ARF2 and its dimerization partners will clarify the mechanism of ARF2 function.

We are grateful to NASC for Col-0, L*er* and Salk_108995 seed (also the Salk Institute for the latter); to Robert Fischer for the GFP_DME_NLS vector; to Bart Janssen (Hort+Research New Zealand) for the BJ36 and BJ40 vectors; to Michael Mogie for assistance with statistical analysis; to Ursula Potter for help with SEM; to Jason Reed for sharing unpublished data; and to Richard Hooley for helpful discussions. M.C.S., M.S., S.T. and N.F. were funded by Sulis Innovation; and S.A. by the BBSRC.

Supplementary material

Supplementary material for this article is available at http://dev.biologists.org/cgi/content/full/133/2/251/DC1

References

Abel, S. and Theologis, A. (1996). Early genes and auxin action. *Plant Physiol.* **111**, 9-17.

Adams, S., Vinkenoog, R., Spielman, M., Dickinson, H. G. and Scott, R. J. (2000). Parent-of-origin effects on seed development in *Arabidopsis thaliana* require methylation. *Development* **127**, 2493-2502.

Alonso, J. M., Stepanova, A. N., Leisse, T. J., Kim, C. J., Chen, H., Shinn, P., Stevenson, D. K., Zimmerman, J., Barajas, P., Cheuk, R. et al. (2003). Genome-wide insertional mutagenesis of Arabidopsis thaliana. *Science* **301**, 653-657.

Alonso-Blanco, C., Blankestijn-De Vries, H., Hanhart, C. J. and Koornneef, M. (1999). Natural allelic variation at seed size loci in relation to other life history traits of *Arabidopsis thaliana. Proc. Natl. Acad. Sci. USA* **96**, 4710-4717.

Baker, S. C., Robinson-Beers, K., Villanueva, J. M., Gaiser, J. C. and Gasser, C. S. (1997). Interactions among genes regulating ovule development in *Arabidopsis thaliana. Genetics* **145**, 1109-1124.

Beeckman, T., De Rycke, R., Viane, R. and Inzé, D. (2000). Histological study of seed coat development in *Arabidopsis thaliana. J. Plant Res.* **113**, 139-148.

Berleth, T. and Jürgens, G. (1993). The role of the *monopteros* gene in organising the basal body region of the *Arabidopsis* embryo. *Development* **118**, 575-587.

Bushell, C., Spielman, M. and Scott, R. J. (2003). The basis of natural and artificial postzygotic hybridization barriers in *Arabidopsis* species. *Plant Cell* **15**, 1-14.

Cheng, W.-H., Taliercio, E. W. and Chourey, P. S. (1996). The *Miniature1* seed locus of maize encodes a cell wall invertase required for normal development of endosperm and maternal cells in the pedicel. *Plant Cell* **8**, 971-983.

Choi, Y., Gehring, M., Johnson, L., Hannon, M., Harada, J. J., Goldberg, R. B., Jacobsen, S. E. and Fischer, R. L. (2002). DEMETER, a DNA glycosylase domain protein, is required for endosperm gene imprinting and seed viability in *Arabidopsis. Cell* **110**, 33-42.

Chojecki, A. J. S., Bayliss, M. W. and Gale, M. D. (1986). Cell production and DNA accumulation in the wheat endosperm, and their association with grain weight. *Ann. Bot.* **58**, 809-817.

Clough, S. J. and Bent, A. F. (1998). Floral dip: a simplified method for *Agrobacterium*-mediated transformation of *Arabidopsis thaliana. Plant J.* **16**, 735-743.

Cui, K.-H., Peng, S.-B., Xing, Y.-Z., Yu, S.-B. and Xu, C.-G. (2002). Molecular dissection of relationship between seedling characteristics and seed size in rice. *Acta Botanica Sinica* **44**, 702-707.

Davies, D. R. (1975). Studies of seed development in *Pisum sativum*. I. Seed size in reciprocal crosses. *Planta* **124**, 303-309.

Davies, D. R. (1977). DNA contents and cell number in relation to seed size in the genus *Vicia. Heredity* **39**, 153-163.

Debeaujon, I., Léon-Kloosterziel, K. M. and Koornneef, M. (2000). Influence of the testa on seed dormancy, germination, and longevity in Arabidopsis. *Plant Physiol.* **122**, 403-413.

Doganlar, S., Frary, A. and Tanksley, S. D. (2000). The genetic basis of seed-weight variation: tomato as a model system. *Theor. Appl. Genet.* **100**, 1267-1273.

Ellis, C. M., Nagpal, P., Young, J. C., Hagen, G., Guilfoyle, T. J. and Reed, J. W. (2005). *AXIN RESPONSE FACTOR1* and *AXIN RESPONSE FACTOR2* regulate senescence and floral abscission in *Arabidopsis thaliana. Development* **132**, 4563-4574.

Garcia, D., Saingery, V., Chambrier, P., Mayer, U., Jürgens, G. and Berger, F. (2003). Arabidopsis *haiku* mutants reveal new controls of seed size by endosperm. *Plant Physiol.* **131**, 1661-1670.

Garcia, D., Fitz Gerald, J. N. and Berger, F. (2005). Maternal control of integument cell elongation and zygotic control of endosperm growth are coordinated to determine seed size in Arabidopsis. *Plant Cell* **17**, 52-60.

Hagen, G. and Guilfoyle, T. (2002). Auxin-responsive gene expression: genes, promoters and regulatory factors. *Plant Mol. Biol.* **49**, 373-385.

Hardtke, C. S. and Berleth, T. (1998). The *Arabidopsis* gene *MONOPTEROS* encodes a transcription factor mediating embryo axis formation and vascular development. *EMBO J.* **19**, 4997-5006.

Harper, J. L., Lovell, P. H. and Moore, K. G. (1970). The shapes and sizes of seeds. *Annu. Rev. Ecol. Syst.* **1**, 327-356.

Harper, R. M., Stowe-Evans, E. L., Luesse, D. R., Muto, H., Tatematsu, K., Watahiki, M. K., Yamamoto, K. and Liscum, E. (2000). The *NPH4* locus encodes the auxin response factor ARF7, a conditional regulator of differential growth in aerial Arabidopsis tissue. *Plant Cell* **12**, 757-770.

Hu, Y., Xie, Q. and Chua, N.-H. (2003). The Arabidopsis auxin-inducible gene *ARGOS* controls lateral organ size. *Plant Cell* **15**, 1951-1961.

Hyten, D. L., Pantalone, V. R., Sams, C. E., Saxton, A. M., Landau-Ellis, D., Stefaniak, T. R. and Schmidt, M. E. (2004). Seed quality QTL in a prominent soybean population. *Theor. Appl. Genet.* **109**, 552-561.

Jofuku, K. D., den Boer, B. G. W., Van Montagu, M. and Okamuro, J. K. (1994). Control of Arabidopsis flower and seed development by the homeotic gene *APETALA2. Plant Cell* **6**, 1211-1225.

Jofuku, K. D., Omidyar, P. K., Gee, Z. and Okamuro, J. K. (2005). Control of seed mass and seed yield by the floral homeotic gene *APETALA2. Proc. Natl. Acad. Sci. USA* **102**, 3117-3122.

Krannitz, P. G., Aarssen, L. W. and Dow, J. M. (1991). The effect of genetically based differences in seed size on seedling survival in Arabidopsis thaliana (Brassicaceae). *Am. J. Bot.* **78**, 446-450.

Krizek, B. A. (1999). Ectopic expression of *AINTEGUMENTA* in *Arabidopsis* plants results in increased growth of floral organs. *Dev. Genet.* **25**, 224-236.

Léon-Kloosterziel, K. M., Keijzer, C. J. and Koornneef, M. (1994). A seed shape mutant of Arabidopsis that is affected in integument development. *Plant Cell* **6**, 385-392.

Leyser, O. (2002). Molecular genetics of auxin signaling. *Annu. Rev. Plant Biol.* **53**, 377-398.

Li, H., Johnson, P., Stepanova, A., Alonso, J. M. and Ecker, J. R. (2004). Convergence of signaling pathways in the control of differential cell growth in *Arabidopsis. Dev. Cell* **7**, 193-204.

Liscum, E. and Briggs, W. E. (1996). Mutations of Arabidopsis in potential transduction and response components of the phototropic signaling pathway. *Plant Physiol.* **112**, 291-296.

Liscum, E. and Reed, J. W. (2002). Genetics of Aux/IAA and ARF action in plant growth and development. *Plant Mol. Biol.* **49**, 387-400.

Lopes, M. A. and Larkins, B. A. (1993). Endosperm origin, development, and function. *Plant Cell* **5**, 1383-1399.

Meyer, R. C., Törjék, O., Becher, M. and Altmann, T. (2004). Heterosis of biomass production in Arabidopsis. Establishment during early development. *Plant Physiol.* **134**, 1813-1823.

Mizukami, Y. and Fischer, R. L. (2000). Plant organ size control: *AINTEGUMENTA* regulates growth and cell numbers during organogenesis. *Proc. Natl. Acad. Sci. USA* **97**, 942-947.

Nagpal, P., Ellis, C. M., Weber, H., Ploense, S. E., Barkawi, L. S., Guilfoyle, T. J., Hagen, G., Alonso, J. M., Cohen, J. D., Farmer, E. E. et al. (2005). Auxin response factors ARF6 and ARF8 promote jasmonic acid production and flower maturation. *Development* **132**, 4107-4118.

Oakenfull, E. A., Riou-Khamlichi, C. and Murray, J. A. H. (2002). Plant D-type cyclins and the control of G1 progression. *Phil. Trans. R. Soc. Lond. B* **357**, 749-760.

Ohto, M., Fischer, R. L., Goldberg, R. B., Nakamura, K. and Harada, J. J. (2005). Control of seed mass by *APETALA2. Proc. Natl. Acad. Sci. USA* **102**, 3123-3128.

Okushima, Y., Overvoorde, P. J., Arima, K., Alonso, J. M., Chan, A., Chang, C., Ecker, J. R., Hughes, B., Lui, A., Nguyen, D. et al. (2005a). Functional genomic analysis of the *AUXIN RESPONSE FACTOR* gene family members in *Arabidopsis thaliana*: unique and overlapping functions of *ARF7* and *ARF19*. *Plant Cell* **17**, 444-463.

Okushima, Y., Mitina, I., Quach, H. L. and Theologis, A. (2005b). AUXIN RESPONSE FACTOR 2 (ARF2): a pleiotropic developmental regulator. *Plant J.* **43**, 29-46.

Przemeck, G. K. H., Mattsson, J., Hardtke, C. S., Sung, Z. R. and Berleth, T. (1996). Studies on the role of the *Arabidopsis* gene *MONOPTEROS* in vascular development and plant cell axialization. *Planta* **200**, 229-237.

Reddy, V. M. and Daynard, T. B. (1983). Endosperm characteristics associated with rate of grain filling and kernel size in corn. *Maydica* **28**, 339-355.

Ruzin, S. E. (1999). *Plant Microtechnique and Microscopy.* Oxford: Oxford University Press.

Schneitz, K., Hülskamp, M. and Pruitt, R. E. (1995). Wild-type ovule development in *Arabidopsis thaliana*: a light microscope study of cleared whole-mount tissue. *Plant J.* **7**, 731-749.

Scott, R. J., Spielman, M., Bailey, J. and Dickinson, H. G. (1998). Parent-of-origin effects on seed development in *Arabidopsis thaliana. Development* **125**, 3329-3341.

Sessions, A., Nemhauser, J. L., McCall, A., Roe, J. L., Feldmann, K. A. and

Zambryski, P. C. (1997). *ETTIN* patterns the *Arabidopsis* floral meristem and reproductive organs. *Development* **124**, 4481-4491.
Sessions, R. A. and Zambryski, P. C. (1995). *Arabidopsis* gynoecium structure in the wild type and in *ettin* mutants. *Development* **121**, 1519-1532.
Skinner, D. J., Hill, T. A. and Gasser, C. S. (2004). Regulation of ovule development. *Plant Cell* **16**, S32-S45.
Smyth, D. R., Bowman, J. L. and Meyerowitz, E. M. (1990). Early flower development in *Arabidopsis*. *Plant Cell* **2**, 755-767.
Stowe-Evans, E. L., Harper, R. M., Motchoulski, A. V. and Liscum, E. (1998). NPH4, a conditional modulator of auxin-dependent differential growth responses in Arabidopsis. *Plant Physiol.* **118**, 1265-1275.
Tian, C., Muto, H., Higuchi, K., Matamura, T., Tatematsu, K., Koshiba, T. and Yamamoto, K. T. (2004). Disruption and overexpression of *auxin response factor 8* gene of *Arabidopsis* affect hypocotyl elongation and root growth habit, indicating its possible involvement in auxin homeostasis in light condition. *Plant J.* **40**, 333-343.
Tiwari, S. B., Hagen, G. and Guilfoyle, T. (2003). The roles of auxin response factor domains in auxin-responsive transcription. *Plant Cell* **15**, 533-543.
Ulmasov, T., Hagen, G. and Guilfoyle, T. (1997). ARF1, a transcription factor that binds to auxin response elements. *Science* **276**, 1865-1868.
Ulmasov, T., Hagen, G. and Guilfoyle, T. (1999a). Activation and repression of transcription by auxin-response factors. *Proc. Natl. Acad. Sci. USA* **96**, 5844-5849.
Ulmasov, T., Hagen, G. and Guilfoyle, T. (1999b). Dimerization and DNA binding of auxin response factors. *Plant J.* **19**, 309-319.
Vandenbussche, F. and Van Der Straeten, D. (2004). Shaping the shoot: a circuitry that integrates multiple signals. *Trends Plant Sci.* **9**, 499-506.
Wang, J.-W., Wang, L.-J., Mao, Y.-B., Cai, W.-J., Xue, H.-W. and Chen, X.-Y. (2005). Control of root cap formation by microRNA-targeted auxin response factors in Arabidopsis. *Plant Cell* **17**, 2204-2216.
Watahiki, M. K. and Yamamoto, K. T. (1997). The *massugu1* mutation of Arabidopsis identified with failure of auxin-induced growth curvature of hypocotyl confers auxin insensitivity to hypocotyl and leaf. *Plant Physiol.* **115**, 419-426.
Weber, H., Borisjuk, L. and Wobus, U. (1996). Controlling seed development and seed size in *Vicia faba*: a role for seed coat-associated invertases and carbohydrate state. *Plant J.* **10**, 823-834.
Wilmoth, J. C., Wang, S., Tiwari, S. B., Joshi, A. D., Hagen, G., Guilfoyle, T. J., Alonso, J. M., Ecker, J. R. and Reed, J. W. (2005). NPH4/ARF7 and ARF19 promote leaf expansion and auxin-induced lateral root formation. *Plant J.* **43**, 118-130.

Table S1. Dimensions of developing seeds in wild-type and *mnt* plants

Stage	Length (μm)		Width (μm)		Area seed cavity (μm²)	
	Wild type	*mnt*	Wild type	*mnt*	Wild type	*mnt*
Preglobular (*n*=16 for wild type, 18 for *mnt*)	325±8	472±20	213±5	279±14	22 187±1046	43 778±4547
Globular (*n*=25 for wild type, 14 for *mnt*)	391±6	533±12	250±4	319±6	30 160±1570	59 857±2436
Heart (*n*=15 for wild type, 16 for *mnt*)	479±7	659±13	327±6	408±8	57 800±2671	106 688±5152
Torpedo (*n*=20 for wild type, 16 for *mnt*)	534±5	708±9	367±5	441±11	86 000±2198	154 125±3453
Bent cotyledon (*n*=11 for wild type, 18 for *mnt*)	542±10	739±11	376±6	482±7	96 091±3206	170 000±5333
Curled cotyledon (*n*=7 for wild type, 28 for *mnt*)	513±8	745±9	369±4	445±10	93 286±4487	170 536±4549

Data represent mean±s.e.m.